17th World Conference on Earthquake Engineering, 17WCEE
Sendai, Japan - September 13th to 18th 2020

EXPERIMETAL STUDY ON FERRO-CEMENT RETROFIT FOR RC FRAME WITH INFILLED BRICK MASONRY WALL

D. Sen[(1)], J. Lamsal[(2)], A. Dutu[(3)], H. Alwashali[(4)], M. Seki[(5)], M. Maeda[(6)]

[(1)] *Ph.D. student, Tohoku University, Japan, dsendip@rcl.archi.tohoku.ac.jp*
[(2)] *Structural Engineer, Bharatpur Metropolitan City, Nepal, jyoti043lamsal@gmail.com*
[(3)] *Lecturer, Technical University of Civil Engineering, Bucharest, Romania, andreea.dutu23@gmail.com*
[(4)] *Assistant Professor, Tohoku University, Japan, hamood@rcl.archi.tohoku.ac.jp*
[(5)] *Visiting Research fellow, Building Research Institute, Japan, sekimatsutaro@yahoo.co.jp*
[(6)] *Professor, Tohoku University, Japan, maeda@rcl.archi.tohoku.ac.jp*

Abstract

Developing countries in earthquake prone regions in the world are still suffering a lot of casualties as well as building damages as observed in recent earthquakes e.g. Nepal earthquake 2015. The damages might be caused by inadequate structural design and/or poor quality control of construction works. Therefore, strengthening of existing buildings are necessary. In general, RC buildings in developing countries contain masonry as a locally available material for partition walls. In order to mitigate strength inadequacy, a strengthening scheme is required that can improve the lateral capacity of masonry infilled RC buildings. For developing countries, due to the lack of skilled workers, an economic and easy to apply retrofit method should be developed based on local materials and construction practices of developing countries in order to accomplish aforementioned goal.

The proposed strengthening solution is Ferro-cement lamination, which refers to a steel wire mesh embedded in mortar layer applied on both sides of masonry wall infilled in RC frame. Ferro-cement has been utilized as a construction as well as a repair material for decades. However, utilization of Ferro-cement as retrofitting material for infilled masonry has not been recognized in building codes due to lacking of comprehensive studies.

This study contains three half scaled RC frames i.e. *i*) Bare frame, *ii*) Masonry infilled RC frame and *iii*) Ferro-cement laminated masonry infilled RC frame. The first objective is to investigate the effect of Ferro-cement lamination on lateral behavior masonry infilled RC frame. The second objective is to propose capacity prediction models in order to evaluate diagonal failure mode of Ferro-cement retrofitted infilled masonry which has been observed in experimental program. In addition, all the specimens have been simulated numerically using macro modelling approach. The experimental results showed that Ferro-cement lamination on infilled masonry can improve the lateral capacity about 1.8 times however with less lateral displacement at peak resistance when compared to masonry infilled RC frame. The proposed lateral capacity evaluation model of diagonal failure mode for the Ferro-cement laminated infilled RC frame can predict lateral capacity with a reasonable agreement with experimental results. Numerical simulation also showed good agreement with the experimental lateral behavior.

Keywords: Ferro-cement; Wire mesh; Infill Masonry; Strengthening; Masonry infilled RC frame

1. Introduction

In developing countries, RC frame structures are very common. Sometimes weak RC frames are designed without considering lateral load and reinforcement ratio and details are not complying with the minimum requirements for structural members. In addition, concrete quality is also poor, in some cases compressive strength could reach 8-10 MPa. Therefore, these buildings with weak reinforced concrete frames are highly vulnerable to severe earthquakes and need to be strengthened to avoid collapse during future earthquakes. Application of existing effective strengthening methods for concrete frames (for example, infilled steel braced frames) is very difficult to execute in developing countries because of the requirement of expertise and expenses. Steel anchors are also necessary to connect the infilled panels to the surrounding frame, that can be hardly installed in low strength concrete. In this respect, an experimental research program was conducted to find low cost strengthening solutions that can be easily applied for weak concrete frames in developing countries. Since, in developing countries, masonry infill panels are used in RC frame as partition wall then strengthening of infill masonry might be a potential solution for seismic strength upgradation. Therefore, in this study Ferro-cement (i.e. which refers to a steel wire mesh embedded in mortar layer applied on both sides of masonry wall infilled in RC frame) was selected for strengthening of masonry infilled RC frame and investigated under lateral cyclic loading.

The primary aim of this study is to experimentally investigate the effect of Ferro-cement lamination on masonry infilled RC frame's lateral resistance and failure mechanism. The second objective is to propose and validate capacity evaluation method of Ferro-cement laminated masonry infilled RC frame based on the observed failure mechanism in the current study. In addition, analytical simulation was done using macro modelling.

2. Experimental program

2.1 Specimen details

The current experimental program consists of three half scaled specimens including a bare RC frame (S1-F), a masonry infilled RC frame (S3-FM), and a Ferro-cement strengthened masonry infilled RC frame (S5-FMFC). This experimental program is a part of the project under Technical University of Civil Engineering of Bucharest (UTCB), Romania focusing on low cost strengthening methods [1]. Details of all specimens are presented in Table 1 and Fig. 1 (a)-(c). The configuration of surrounding RC frame of all specimens are same as shown in Fig. 1(a). After the bare RC frames construction, two RC frames were infilled with masonry. The masonry panel was built inside the RC frame, with burned solid clay bricks of 240x115x63 mm available in Romanian market, in running bond manner. After that, one masonry infilled RC frame was wrapped with Ferro-cement lamination. In the Ferro-cement lamination, wire mesh having 0.9mm diameter wires at a spacing of 13 mm in both directions was used. Initially two layers of wire meshes were attached with masonry and RC frame with clamp and nails, respectively. After that a 20mm mortar layer was applied on the wire mesh wrapped on overall RC frame and masonry.

Table 1 - Details of all specimens

Specimen	*RC column*		*Masonry*	*Ferro-cement*			
	Dimension	Main reinforcement	Thickness t_{mas}	Thickness t_{FC}	Wire diameter φ_{wm}	Wire spacing s	Number of mesh layers
	mm		(mm)	(mm)	(mm)	(mm)	
S1-F			-	-	-	-	-
S3-FM	250 x 250	4-φ12mm	115	-	-	-	-
S5-FMFC			115	20	0.9	13	2

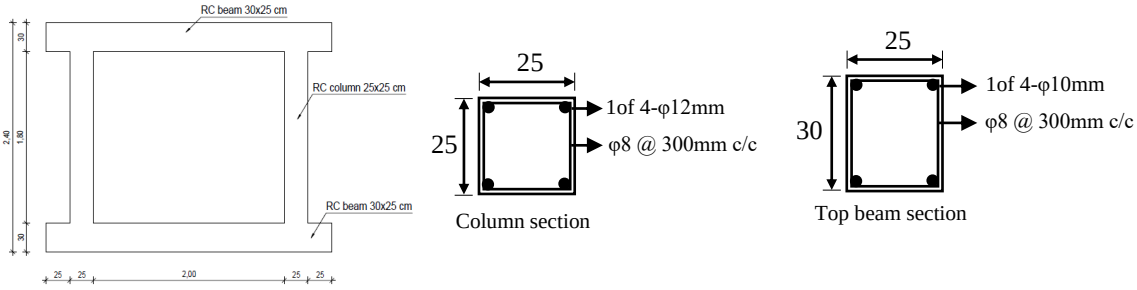

(a) Reinforced concrete (RC) frame (S1-F)

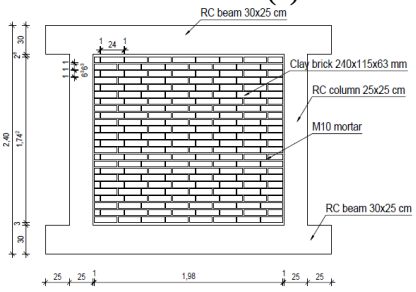

(b) Masonry infilled RC frame (S3-FM)

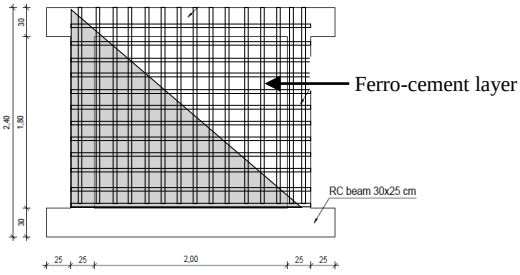

(c) Ferro-cement laminated masonry infilled RC frame (S5-FMFC)

Fig. 1- Dimension and reinforcement detailing of test specimens (*dimensions are in cm*)

2.2 Material properties

Material properties of concrete and reinforcing steels used in the specimens are shown in Table 2. The material properties of masonry and Ferro-cement coating are shown in Table 3. Solid burnt clay brick of 41MPa compressive strength was used for masonry construction. For masonry construction and Ferro-cement coating readily mixed dry mortar was used. The average compressive strength of masonry joint mortar and Ferro-cement coating, mortar are presented in Table 3. The wire mesh was tested as per ACI 549 [2]; however, the yield strength of wire could not be identified by material test. Therefore, the yield strength of wire mesh has been considered as $f_{y,wm} = 0.71 f_{u,wm}$ as per AS/NZS [3], where $f_{y,wm}$, $f_{u,wm}$ = yield and ultimate strength of wire mesh, respectively.

Table 2- Material Properties for concrete and steel (all values are in MPa)

Specimen	Concrete	Reinforcement					
		Φ8		Φ10		Φ12	
	$f_{c'}$	f_y	f_{ult}	f_y	f_{ult}	f_y	f_{ult}
S1-F S3-FM S5-FMFC	14	364	429	454	553	428	525

$f_{c'}$ = concrete compressive strength, f_y, f_{ult} = yield and ultimate strength of reinforcement

Table 3- Material Properties for masonry and ferro-cement coating (all values are in MPa)

Specimen	Masonry		Ferro-cement		
			Mortar	Wire mesh	
	f_m	$f_{mor,j}$	$f_{mor,FC}$	$f_{u,wm}$	$f_{y,wm}$
S1-F	-	-	-	-	-
S3-FM	11.6	6.1	-	-	-
S5-FMFC	11.6	8.8	4.8	629	447

f_m= masonry compressive strength; $f_{mor,j}$, $f_{mor,FC}$ = mortar compressive strength of joint and Ferro-cement mortar; $f_{y,wm}$, $f_{u,wm}$ = yield and ultimate strength of wire mesh.

2.3 Instrumentation and loading system

All the specimens were subjected to cyclic lateral loading and constant axial load of 350 kN on each column in the reaction frame in UTCB donated by JICA, as shown in Fig. 2. Two pantographs have been used to avoid any out-of-plane movement of the frame during loading. The cyclic lateral loading program consisted of two cycles for each lateral drift of 0.0625, 0.125, 0.25, 0.50, 1.0, 1.5, 2.0, and 3.0 % as shown in Fig. 3. The lateral drift is defined as the ratio of top lateral displacement, measured at the center of beam, to the height of column taken from the top of foundation beam to center of top beam. The average lateral top displacement has been recorded using LVDTs attached at the center of top beam.

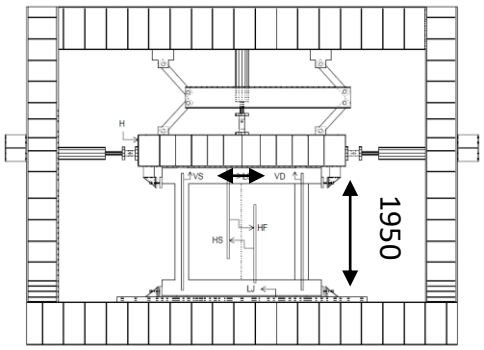

Fig. 2- Test setup on the reaction frame

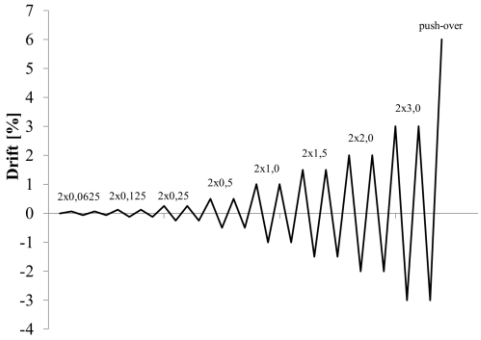

Fig. 3- Loading protocol

3. Experimental results

3.1 Lateral behavior and failure mechanism

3.1.1 Bare RC frame (S1-F)

The lateral cyclic behavior of specimen S1-F is shown in Fig. 4(a). At first, flexural crack appeared on the top beam at 0.25% story drift. After that, the crack width increased gradually and the beam yielded at about 0.5% story drift. Following the beam's yielding, load redistribution happened, therefore flexural cracks on the tension column appeared. The maximum lateral resistance, 81kN, occurred at 1% story drift. After peak resistance, crack width of column increased gradually that caused concrete spalling at about 2% story drift. The specimen failed by flexural hinge formation at column top and bottom at 2% story drift in negative cycle. Further it was loaded up to negative 3%, at this stage the damage is shown in Fig. 5(a).

3.1.2 Masonry infilled RC frame (S3-FM)

The lateral cyclic behavior of specimen S3-FM is shown in Fig. 4(b). Initially, diagonal stepped cracks formed near both ends of the masonry strut, i.e. loaded diagonal, at 0.25% story drift. At 0.5% story drift, several flexural cracks appeared at the top of tension column. In addition, the steeped diagonal cracks, appeared in the previous cycle, tried to propagate towards center of the diagonal and several horizontal sliding plane formed on masonry. The maximum lateral resistance was 191 kN at about negative 1% story drift, where infill masonry slide through the horizontal cracks, and shear cracks appeared on the top of tension columns. At 1.5~2.0% story drift, all the cracks on tension column opened largely causing concrete spall off and at the same stages infill masonry slide through previously formed cracks. The masonry infilled RC frame, failed at about negative 3% story drift, with the loss of the axial force carrying capacity caused by the shear failure at the bottom of the columns as shown in Fig. 5(b).

3.1.3 Ferro-cement laminated masonry infilled RC frame (S5-FMFC)

The lateral cyclic behavior of specimen S5-FMFC is shown in Fig. 4(c). In contrast to masonry infilled RC frame (S3-FM), first flexural crack appeared early on bottom of tension column at 0.125% story drift. At negative 0.21% story drift, maximum lateral resistance of 330kN occurred with several diagonal cracks formed

on the loaded diagonal of FC laminated masonry as shown in Fig. 5(c). After peak resistance, the load transfer mechanism of FC laminated infill changed to sliding mechanism which is evident from the sliding of infill panel at 0.5% story drift. The influence of sliding could also be seen from the shape of larger hysteresis loops after 0.5% story drift as shown in Fig. 4(c). The sliding was significantly observed on two horizontal plane as shown in Fig. 5(c) at -1.5% story drift, which created three panels which pushed the columns and distributed damages along height, rather than concentrating them at bottom of column. Following the sliding of infill panel, the specimen S5-FMFC failed at negative 1.5% drift, as shown in Fig. 5(c), due to shear failure at the upper part of the tension column.

3.2 Comparison of lateral behavior

For the comparison of lateral behavior, experimental backbone curves of all the specimens are shown in Fig. 6. The bare RC frame (S1-F) showed maximum lateral resistance of 81kN and -79kN at 1.0% and -1.5% story drift, respectively.

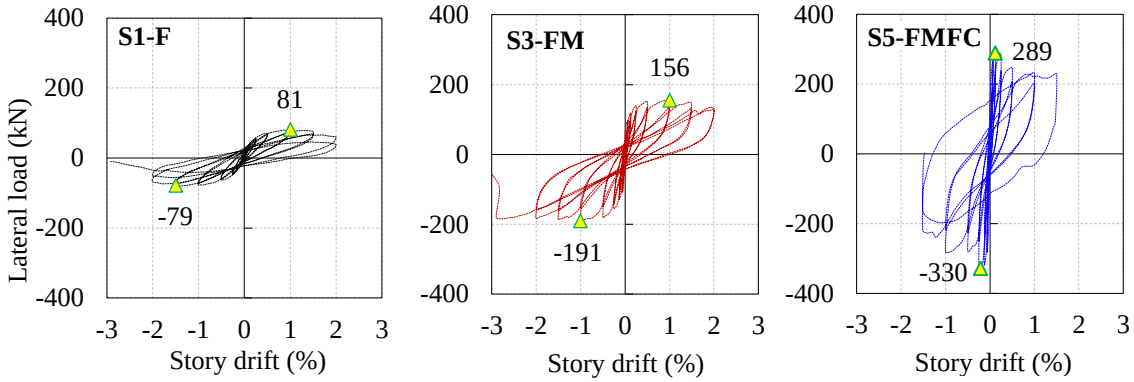

(a) (b) (c)

Fig. 4- Lateral load vs. story drift graphs of specimen (a) S1-F, (b) S3-FM and (c) S5-FMFC

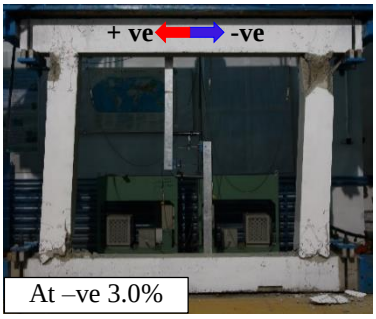

a) Bare Frame (S1-F)

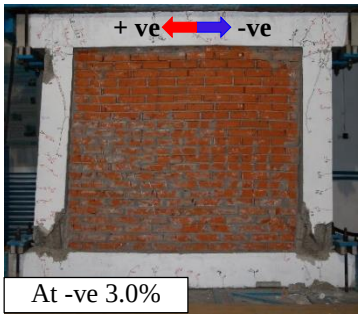

b) Masonry infilled RC Frame (S3-FM)

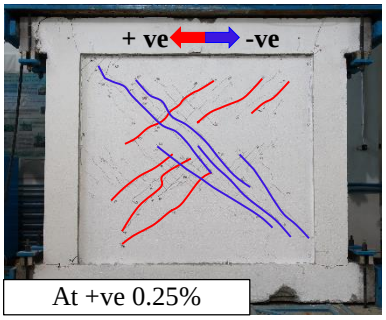

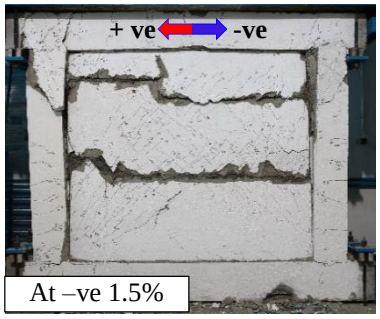

c) Ferro-cement laminated masonry infilled RC Frame (S5-FMFC)

Fig. 5- Observed damages of specimen (a) S1-F, (b) S3-FM and (c) S5-FMFC

The story drift at 80% of maximum capacity is about 1.9% which indicates a very ductile behavior. Insertion of masonry wall essentially improved the lateral resistance to 156 kN and -191 kN at 1.0% and -1.0% story drift, respectively, which is 2.2 time greater that bare frame capacity. The story drift at 80% of maximum capacity is about 2% which indicates a relatively ductile behavior which can be attributed to the sliding of infill masonry. Further, FC laminated masonry infilled RC frame (S5-FMFC) showed maximum lateral resistance of 289 kN and -330 kN at 0.12% and -0.21% story drift, respectively, which is about 1.8 times greater that masonry infilled RC frame's (S3-FM) lateral capacity. The peak resistance at lower story drift can be attributed to the higher stiffness and strength of the FC laminated masonry infill compared to infill masonry. However, the story drift at 80% of maximum capacity is about 1.1% which indicates relatively less ductile behavior than bare frame and masonry infilled RC frame. Therefore, from this experimental observation, it can be concluded that Ferro-cement can be used to strengthen infill masonry when strength upgradation is the primary concern rather than both strength and ductility.

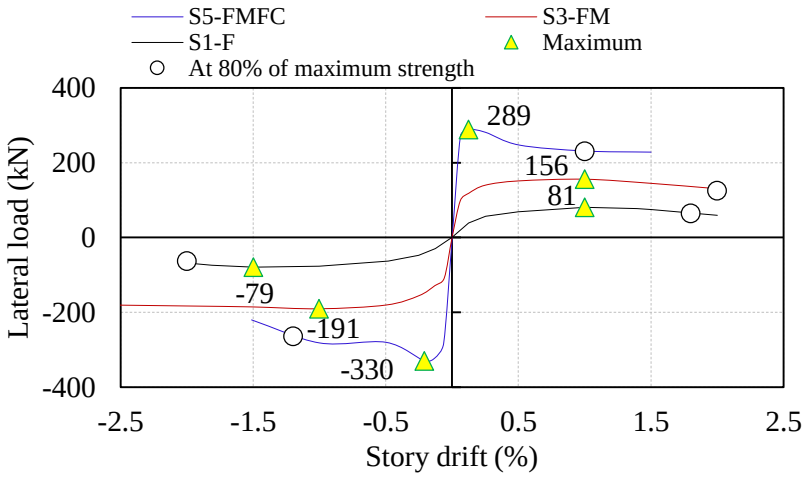

Fig. 6- Lateral load-story drift backbone curves of all specimen

4. Lateral capacity evaluation

4.1 Capacity evaluation of bare frame (S1-F)

Bare frame capacity has been evaluated considering flexural hinge formation at the top and bottom of frame because the RC column was designed as flexural column. The moment capacity of top hinge has been considered as the minimum of beam and column capacity. The lateral capacity can be calculated as per JBDPA [4], using Eq. (1) to Eq. (2).

$$Q_{fr} = 2 \text{ x } Q_{mu} \tag{1}$$

$$Q_{mu} = \frac{M_u + M_b}{h_o} \tag{2}$$

where, Q_{fr} = bare RC frame capacity, Q_{mu}= shear capacity of column at flexural yielding, M_u = minimum of the ultimate moment capacities of beam and column at top joint, M_b = ultimate moment capacity of column, and h_o = clear height of column.

4.2 Capacity evaluation of masonry infilled RC frame (S3-FM)

Lateral strength of masonry infilled RC frame is considered as the summation of RC frame capacity and infill masonry lateral capacity as per Eq. (3).

$$Q_{S3-FM} = Q_{fr} + Q_{mas} \tag{3}$$

where, Q_{S3-FM} = lateral strength of masonry infilled RC frame, Q_{fr} = bare RC frame capacity, Q_{mas} = lateral capacity of infill masonry.

The lateral capacity of masonry infill (Q_{mas}) has been evaluated considering minimum of sliding ($Q_{mas,slide}$) and diagonal compression ($Q_{mas,comp.}$) capacities. In general, diagonal strut forms on infill masonry just after the separation of RC frame and infill masonry. However, the final failure could be diagonal crushing, sliding or combination depending on the masonry properties and frame-masonry interaction. The lateral capacity of infill during sliding is calculated considering Eq. (4), as proposed by Pauley and Priestley [5].

$$Q_{mas,slide} = \left(\frac{\tau_0}{1-\mu\ tan\theta}\right) L t_{mas} \tag{4}$$

where, τ_o = cohesion capacity of infill masonry that has been proposed by Pauley and Priestley [5] as $0.03f_m$, μ = frictional coefficient (= 0.3), θ = angle of diagonal with horizontal, L = length of masonry and t_{mas} = thickness of masonry.

In case of diagonal compression failure, a diagonal strut is considered to be formed and eventually crushed inside the RC frame. The strut width has been calculated using Eq. (5) - Eq. (6) as proposed by Mainstone [6], which is also suggested by FEMA 306 [7]. The lateral capacity of masonry infill is considered as the horizontal component of diagonal strut capacity as Eq. (7).

$$W_s = 0.175(\lambda_1 h)^{-0.4} d_m \tag{5}$$

$$\lambda_1 = \sqrt[4]{\frac{E_{mas} t_{mas} sin2\theta}{4 E_c I_c h_o}} \tag{6}$$

$$Q_{mas,comp} = f_{m,90} W_s t_{mas} cos\theta \tag{7}$$

where, W_s = width of masonry strut, λ_1 = stiffness parameter, h = height of column at the center of beam, d_m = diagonal length of masonry infill, $f_{m,90}$ = compressive strength of masonry in horizontal direction (=$0.5f_m$ as suggested by FEMA 306 [7]), f_m = compressive strength of masonry prism, E_{mas}/E_c = Young's modulus of masonry/concrete, t_{mas} =thickness of masonry, I_c = moment of inertia of column, h_o = clear height of column, and θ = angle of diagonal with horizontal.

In addition, Alwashali et al. [8] proposed a simple empirical approach to evaluate the capacity of infill masonry considering both failure modes i.e. sliding and diagonal compression failure. In that study [8] the lateral capacity of infill masonry has been proposed as Eq. (8)

$$Q_{mas} = 0.05 f_m L t_{mas} \tag{8}$$

where, f_m = compressive strength of masonry prism, L= length of masonry and t_{mas}= thickness of masonry. The lateral capacity of infill masonry has been considered as the minimum of the computed capacities from Eq. (4), Eq. (7), and Eq. (8). The computed values will be discussed in section 5.

4.3 Capacity evaluation of FC laminated masonry infilled RC frame (S5-FMFC)

The schematic diagram of the observed failure mechanism of FC laminated masonry infilled RC frame is shown in Fig.7(a). The FC laminated masonry cracked on the loaded diagonal direction whereas the frame behaves like bare frame i.e. hinges at ends of top beam and bottom of columns. Lateral capacity of the observed failure has been evaluated by Eq. (9). The lateral strength of RC frame (Q_{fr}) has been computed by Eq. (1) as discussed in the earlier subsection.

$$Q_3 = Q_{fr} + Q_{wall} \tag{9}$$

where, Q_{fr} = lateral capacity of RC frame, and Q_{wall} = lateral strength of FC laminated infill masonry.

At diagonal cracking, lateral strength of FC laminated masonry (Q_{wall}) can be evaluated as a summation of the contribution of masonry and wire meshes using Eq. (10). The contribution of FC layer mortar in cracking has not been considered assuming the fact that the mortar and wire mesh will not work together because FC layer mortar would crack before wire meshes comes into tension.

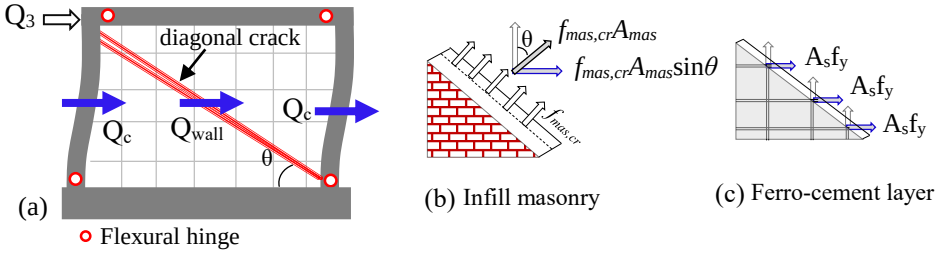

Fig. 7 – (a) Schematic diagram of diagonal cracking failure, (b) cracked infill masonry and (c) cracked Ferro-cement layer

$$Q_{wall} = Q_{mas,cr} + Q_{FC,wm} \tag{10}$$

where, Q_{wall} = lateral capacity of FC laminated masonry wall, $Q_{mas,cr}$ = horizontal component of diagonal cracking capacity of masonry, and $Q_{FC,wm}$ = lateral strength wire meshes in FC layer. The evaluation of masonry and FC layer strength at diagonal cracking is discussed in following subsections.

4.3.1 Masonry diagonal cracking capacity ($Q_{mas,cr}$)

The contribution of infill masonry due to diagonal cracking has been evaluated using Eq. (11), in reference to Fig. 7(b).

$$Q_{mas,cr} = f_{mas,cr} A_{mas} sin\theta \tag{11}$$

where, $f_{mas,cr}$ = cracking strength of infill masonry, A_{mas} = diagonal area of infill masonry (diagonal length x thickness), θ = angle of diagonal with horizontal.

Masonry diagonal cracking strength ($f_{mas,cr}$) is explained in reference to diagonal masonry wallet test as shown in Fig. 8(a). Under diagonal loading (P_d), the center of masonry wallet is in pure shear state and generally the crack is formed in loaded diagonal direction. The formation of diagonal crack is due to tension as explained in Fig.8(a) through stress transformation. The Mohr's circle of the stress transformation is also shown in Fig. 8(b) from where it is evident that shear stress should be equal to principal normal stresses (σ_1 and σ_2). At diagonal cracking, shear strength ($\tau_{d,mas}$) should be equal to the tensile strength ($f_{mas,cr}$) of masonry. Therefore, the cracking strength has been evaluated from diagonal masonry wallet test. Several diagonal test of masonry wallet [9-23] have been investigated to correlate shear strength of masonry i.e. cracking strength with masonry compressive prism strength. The correlation is shown in Fig. 9 and the diagonal shear strength (as well as diagonal cracking strength, $f_{mas,cr}$) can be considered as $0.05f_m$ by linear regression with correlation coefficient of 0.55.

4.3.2 Contribution of wire mesh ($Q_{FC,wm}$)

The contribution of Ferro-cement has been considered to be equal to shear capacity provided by the

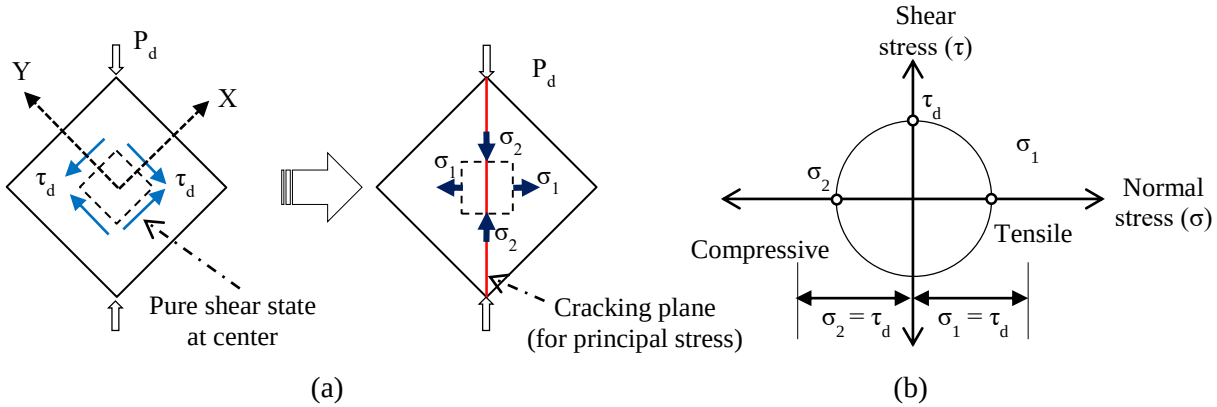

Fig. 8- a) State of stress on diagonal wallet and b) Corresponding Mohr's circle representation

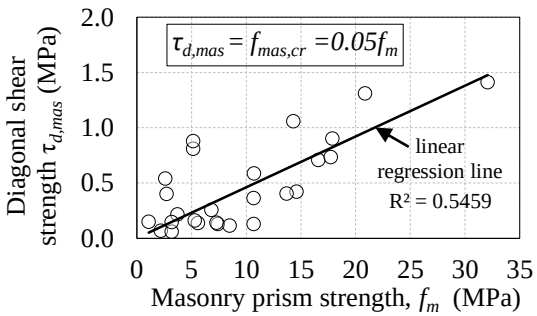

Fig. 9-Relationship between diagonal shear strength and masonry prism strength

horizontal mesh reinforcements using Eq. (12) in reference to Fig. 7(c). However, an empirical reduction factor (α) has been imposed in the contribution of wire mesh, in Eq. (12), to accommodate less effectiveness of mesh reinforcement compared to contribution in RC shear wall. The less effectiveness might happen because wires are not embedded in RC frame as in shear wall. In this study, the empirical reduction factor has been considered as 0.7 for Ferro-cement lamination as proposed by Sen et al. [24]

$$Q_{FC,wm} = \alpha n_s n_L \left(\frac{h_{mas}}{s}\right) A_s f_{y,wm} \tag{12}$$

where, n_s = number of surface retrofitted with FC, n_L =number of wire mesh layer in each FC layer, h_{mas} = height of masonry infill, s = spacing of horizontal mesh reinforcements, A_s = area of horizontal wire, $f_{y,wm}$ = yield tensile strength of wire mesh, and α = empirical reduction factor (= 0.7).

5. Validation of lateral capacity evaluation

The computed component capacities of bare frame (S1-F), masonry infilled RC frame (S3-FM) and Ferro-cement laminated masonry infilled RC frame (S5-FMFC) are reported in Table 4 and also shown in Fig. 10(a)-(c). The calculated bare frame (S1-F) capacity, as shown in Fig. 10(a), shows good agreement with experimental lateral maximum resistance, with calculated to experimental capacity (average of both direction) ratio of 0.88.

As discussed in the earlier section, for specimen S3-FM, lateral capacity of surrounding frame has been considered same as bare frame. However, lateral capacity of infill masonry would be the minimum of sliding and diagonal compression capacities. Alwashali et al. [8] suggested an empirical infill masonry capacity

Table 4- Calculated strength of all test specimens

Component (*All capacities are in kN*)		Specimen		
		S1-F	***S3-FM***	***S5-FMFC***
RC frame	Lateral capacity due to flexural hinge [Eq. (1)]	70	70	70
Masonry	Simplified [Eq. (8)]	-	134	-
	Sliding [Eq. (4)]	-	110	-
	Diagonal compression [Eq. (7)]	-	139	-
	Diagonal cracking [Eq. (11)]	-	-	121
Ferro-cement	Wire mesh [Eq. (12)]	-	-	110
Calculated capacity		70	*180	301
Experimental capacity (avg. of +ve and –ve loading)		80	173	309
Predicted / Experimental		0.88	0.96	0.97

* Summation of RC frame capacity and minimum of simplified, sliding and diagonal compression capacity of masonry

prediction model which accommodates both failure modes and, by using it, the total capacity of masonry infilled RC frame resulted as 204 kN, which is 18% greater than the experimental capacity of 173 kN (average of both loading direction). In addition, the sliding and diagonal compression capacities of infill masonry have been evaluated as per Pauley and Priestley [6] and FEMA 306 [7], respectively. From calculated values in Table 4, it is clear that sliding capacity of infill masonry is less than the diagonal compression capacity, hence the failure should be by sliding of infill masonry which resembles with the damage observation of experimental failure mode. The predicted lateral strength, 180 kN as shown in Fig. 10(b), of masonry infilled RC frame (S3-FM) considering sliding failure of infill shows fair agreement with experimental lateral maximum resistance with calculated to experimental capacity (average of both direction) ratio of 0.96. The failure mechanism of FC laminated masonry infilled RC frame (S5-FMFC) has been found as diagonal cracking of FC strengthened infill masonry. The diagonal cracking of capacity masonry and wire mesh contribution are added to bare frame capacity. The evaluated lateral capacity has been evaluated as 301 kN as shown in Fig. 10(c), with calculated to experimental capacity (average of both direction) ratio of 0.97.

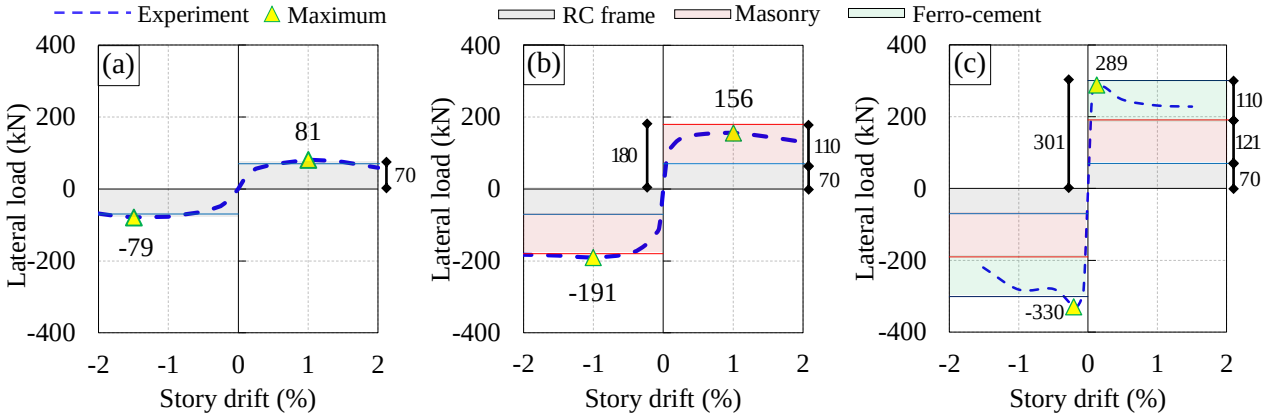

Fig. 10 – Comparison of calculated and experimental strength of (a) bare frame, (b) masonry infilled RC frame and (c) FC laminated masonry infilled RC frame.

6. Nonlinear pushover analysis

6.1 Modelling of specimen

For strength based design, above mentioned capacity evaluation is necessary. However, for performance based design it is necessary to have a complete lateral behavior of structure. Therefore, attempt has been taken to model the specimen S1-F, S3-FM and S5-FMFC in ETABS. In all models, RC frame has been considered with nonlinear flexural hinges properties (M/M_y), as shown in Fig. 11(a)-(b), on both ends of columns and beam. In the masonry infilled RC frame model (S3-FM), infill masonry has been modeled as an equivalent strut having axial capacity of $Q_{axial,mas}$ that has the horizontal component ($Q_{axial,mas}\ cos\theta = Q_{mas,slide}$) of 110 kN reflecting the sliding capacity (Eq. (4)) as shown in Table 4. In the modelling of FC laminated masonry infilled RC frame (S5-FMFC) infill masonry and FC layer have been modeled as two different equivalent struts in RC frame. The infill masonry has been modeled as equivalent strut having axial capacity ($Q_{axial,mas}$) that has horizontal component ($Q_{axial,mas}cos\theta = Q_{mas,cr}$) of 121 kN reflecting the diagonal cracking capacity (Eq. (11)) as shown in Table 4.

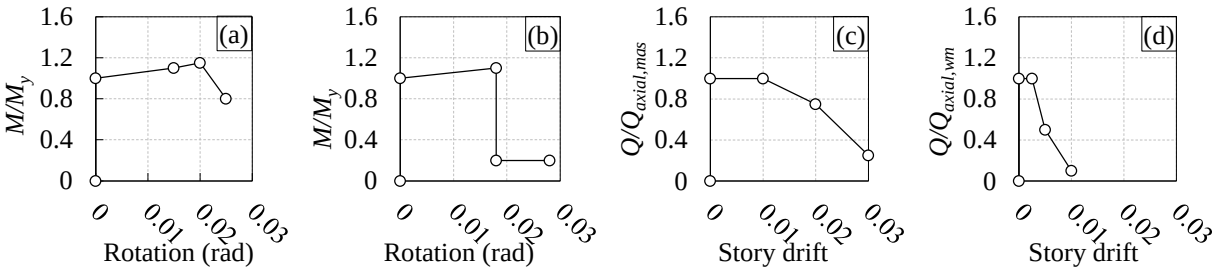

Fig. 11 – Non-linear hinge properties of (a) RC column, (b) RC beam, (c) masonry of S3-FM, and (d) FC of S5-FMFC

In addition, the Ferro-cement layer has been modeled as strut having axial capacity ($Q_{axial,wm}$) that has horizontal component ($Q_{axial,wm}cos\theta = Q_{FC,wm}$) of 110kN reflecting the shear capacity of wire meshes in FC (Eq. (12)) as shown in Table 4. It is to be noted that the contribution of wire mesh has been considered as strut to make the model simple enough to accommodate the shear capacity of wire mesh in ETABS. The deformation capacities of masonry and FC have been considered in accordance to the experimental observation as shown in Fig. 11(c)-(d). After modelling, pushover analysis has been executed using ETABS.

6.2 Comparison with experimental observation

The numerical analysis results i.e. hinge formation, bending moment diagram and axial force are shown in Fig. 12-14. From Fig. 12 and 14, it is evident that for all specimens- the moment concentrated at the top and bottom joints of RC frame and the plastic hinges formed at the ends of top beam and bottom of columns. However, in the experiment the damage occurred initially on the beam and then concentrated to the column through load redistribution. In the case of specimen S3-FM and S5-FMFC, peak lateral resistance associated with axial force on diagonal strut which is close to axial capacity as shown in Fig.13 (b) and (c) and axial hinge formation on the diagonal struts, as shown in Fig.14 (b) and (c).

The experimental and numerical lateral capacity curves are compared in Fig. 15. From the comparison, it is evident that the overall lateral behavior of bare frame (S1-F), masonry infilled RC frame (S3-FM), and FC laminated masonry infilled RC frame (S5-FMFC) can be estimated using numerical analysis. The ratio of calculated to experimental capacities are 0.86, 0.97 and 0.90 for bare frame (S1-F), masonry infilled RC frame (S3-FM), and FC laminated masonry infilled RC frame (S5-FMFC), respectively, which indicates a good agreement with experimental results.

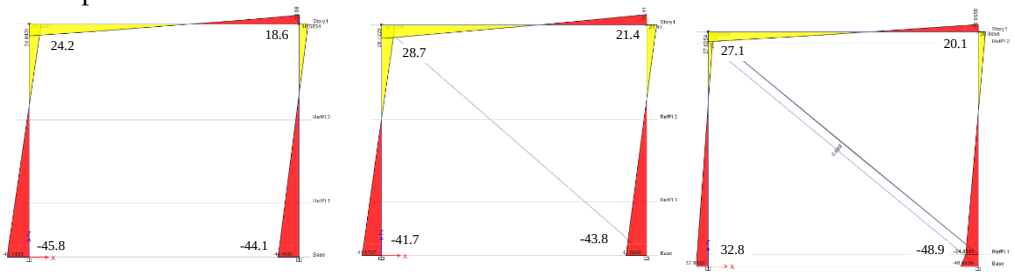

(a) (b) (c)

Fig. 12 – Bending moment (kN-m) diagrams at peak resistance of specimen (a) S1-F, (b) S3-FM, and (c) S5-FMFC

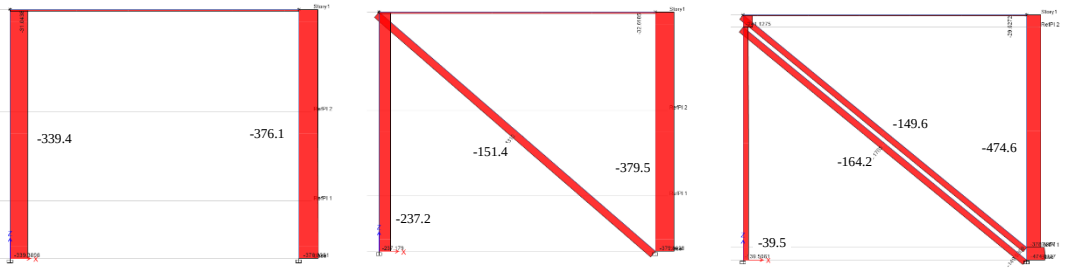

(a) (b) (c)

Fig. 13 – Axial force (kN) at peak resistance of specimen (a) S1-F, (b) S3-FM, and (c) S5-FMFC

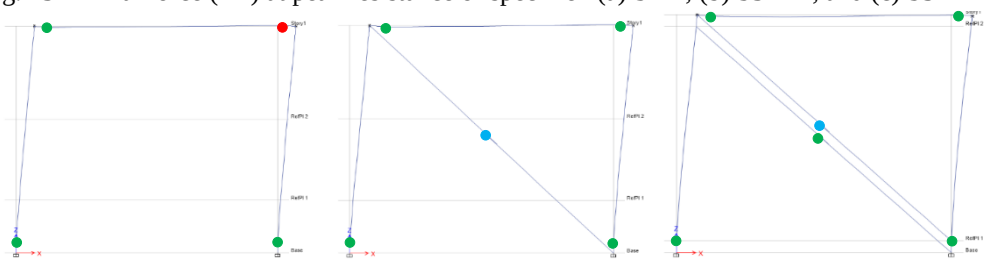

(a) (b) (c)

Fig. 14 – Hinge locations of specimen (a) S1-F, (b) S3-FM, and (c) S5-FMFC

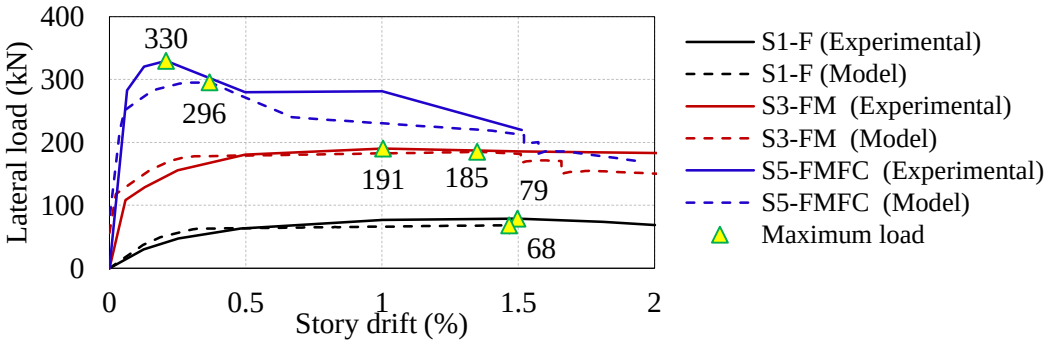

Fig. 15 – Comparison of lateral capacity curves of specimen (a) S1-F, (b) S3-FM, and (c) S5-FMFC

7. Conclusions

In this study, experiments have been conducted on bare RC frame, masonry infilled RC frame and Ferro-cement laminated masonry infilled RC frame to investigate lateral behavior and to analyze lateral strength based on the observed failure mechanism. In addition, numerical model has also been developed using macro modeling technique. The following conclusions can be drawn from this study:

a) The Ferro-cement lamination on infilled masonry improved lateral capacity about 1.8 times when compared with masonry infilled RC frame. Ferro-cement lamination changed load transfer mechanism of infill panel from sliding to diagonal cracking keeping similar behavior of RC frame at peak resistance.
b) Capacity evaluation method for FC laminated infilled masonry has been proposed. The proposed capacity evaluation for Ferro-cement laminated masonry infilled RC frame demonstrated a good agreement having calculated to experimental capacity ratio of 0.9.
c) The lateral behavior of the RC frame, the RC frame infill masonry and the Ferro-cement laminated masonry infilled RC frame can be simulated numerically with fair agreement.

8. References

[1] Seki M, Popa V, Lozinca E, Dutu A, Papurcu A (2018): Experimental Study on Retrofit Technologies for RC Frames with Infilled Brick Masonry Walls in Developing Countries. *In 16th European Conference on Earthquake Engineering*, Greece.
[2] ACI 549 1R-93 (1993): *Guide for the Design, Construction and Repair of Ferro-cement* (Reapproved 1999).
[3] AS/NZS 4671 (2001): *Steel reinforcing materials*.
[4] *Standard for seismic evaluation of existing concrete buildings* (2001): Japan Building Disaster Prevention Association.
[5] Paulay T, Priestley MJN (1992): *Seismic design of reinforced concrete and masonry buildings*. Wiley, New York
[6] Mainstone RJ (1971): On the stiffness and strength of infilled frames. *Proc. of the Institution of Civil Engineers*, **49**(2), 230.
[7] FEMA 306 (1998): *Evaluation of earthquake damaged concrete and masonry wall buildings*. Applied Technology Council
[8] Alwashali H, Suzuki Y, Maeda M (2017): Seismic evaluation of reinforced concrete buildings with masonry infill. *Proc. of 16th WCEE*, Chile.
[9] Mustafaraj E, Yardım Y (2016): Usage of Ferro cement jacketing for strengthening of damaged unreinforced masonry (URM) walls. *3rd International Balkans Conference on Challenges of Civil Engineering*, Epoka University, Tirana, Albania
[10] Prawel SP, Reinhorn AM, Quzi SI (1989): Upgrading the seismic resistance of unreinforced brick masonry using Ferro cement coatings, *Proceedings 8th International Brick/Block Masonry Conference*, Dublin, Ireland.
[11] Kadam SB, Singh Y (2012): Mechanical properties of externally strengthened masonry. *In Proc. of 15th WCEE*, Lisbon, Portugal.
[12] Demirel IO, Yakut A, Binici B, Canbay E (2015): Experimental investigation of infill behaviour in RC frames. *Proc. of 10th PCEE, Australia*.
[13] Shermi C, Dubey RN (2018): In-plane behaviour of unreinforced masonry panel strengthened with welded wire mesh and mortar. *Construction and building materials*, 178, 195-203.
[14] Russell A (2010): *Characterisation and seismic assessment of unreinforced masonry buildings* (Doctoral dissertation, Auckland).
[15] Dizhur D, Ingham JM (2013): Diagonal tension strength of vintage unreinforced clay brick masonry wall panels. *Cons. and Build Mat.*, **43**.
[16] Lin YW, Wotherspoon L, Scott A, Ingham JM (2014): In-plane strengthening of clay brick unreinforced masonry wallettes using ECC shotcrete. *Engineering Structures*, **66**, 57-65.
[17] Wang X, Lam CC, Iu VP (2018). Experimental investigation of in-plane shear behaviour of grey clay brick masonry panels strengthened with SRG. *Engineering Structures*, **162**, 84-96.
[18] Ouyang Y, Pam HJ, Lo SH, Wong YL, Li J (2012): Preliminary study of masonry-RC hybrid structure behavior under earthquake loading. *In Proc. of 15th WCEE*, Lisbon, Portugal.
[19] Petersen RB (2009): *In-plane shear behaviour of unreinforced masonry panels strengthened with fibre reinforced polymer strips* (Doctoral dissertation, University of Newcastle).
[20] Morandi P, Milanesi RR, Magenes G (2016): Innovative seismic solution for clay masonry infills with sliding joints: principles and details. *In Proceedings of 16th International Brick and Block Masonry Conference*, Italy.
[21] Bustos-García A, Moreno-Fernández E, Zavalis R, Valivonis J (2019): Diagonal compression tests on masonry wallets coated with mortars reinforced with glass fibers. *Materials and Structures*, **52**(3), 60.
[22] Malyszko L (2004): In-plane shear and tensile strength tests of small brickwork specimens. *Proceedings of the 4th Int. Sem. on Structural Analysis of Historical Constructions*, Italy.
[23] Dehghani A, Fischer G, Alahi FN (2015): Strengthening masonry infill panels using engineered cementitious composites. *Materials and Structures*, **48**(1-2), 185-204.
[24] Sen D, Alwashali H, Islam MS, Maeda M (2020): Investigation of the lateral capacity of Ferro-cement retrofitted infilled masonry in RC frame and simplified prediction approach. *AIJ Journal of Technology and Design*, **26**(62), 159-163.

